A METAMATERIAL-BASED *E*-PLANE HORN ANTENNA

R.-B. Hwang, H.-W. Liu, and C.-Y. Chin

Department of Electrical Engineering
National Chiao-Tung University
1001, Da-Hsueh Road, 300 Hsinchu, Taiwan, Republic of China

Abstract—In this paper, we reported an *E*-plane horn antenna incorporating a metamaterial. Such a metamaterial is made up of metallic cylinders organized in a two-dimensional square lattice. After properly designing the lattice constant and unit cell pattern, we synthesized a medium with the effective refractive index smaller than unity. Therefore, once the waves were excited within the metamaterial, the refractive waves tend to be perpendicular to the interface between the metamaterial and uniform medium. Based on this concept, a 4-way beam splitter was designed to equally distribute the input power into 4 different directions. We then guide each of the power into individual *E*-plane flared opening to radiate a directional beam pattern in each sector. We have fabricated this antenna and measured its radiation characteristics including the return loss and far-field pattern. The excellent agreement between the measured and simulated results was obtained. Due to the properties of robust, low-loss, and low-cost, this antenna may have promising application in a point-to-multiple-point downlink system.

1. INTRODUCTION

This research demonstrates a new *E*-plane horn antenna radiating four directional beam patterns over the four sectors. Specifically, the multi-beam characteristic was due to the extraordinary properties of wave propagating in a metamaterial inserted in a radiating structure to be presented in this paper. Metamaterial is an artificial material which obtains its properties from its structure instead of directly from its composition [1, 2]. In general, a metamaterial is synthesized

Corresponding author: R.-B. Hwang (raybeam@mail.nctu.edu.tw).

by embedding specific inclusions, for example, periodic structures, in a host medium. So far, a rich variety of metamaterials were invented, and their basic physical mechanism was studied thoroughly using experimental or theoretical way [1–16]. To mention a few, the characteristics of electromagnetic wave propagating in anisotropic left-handed materials were investigated [3, 4]. The metamaterial made up of wire medium was intensively studied, particularly on its effective refractive index, permittivity and permeability. Specifically, the structure composed of metallic mesh wires, which has very small electrical length in the period and wire thickness, is characterized as a homogeneous medium with a low plasma frequency [5, 6]. Pendry et al. [5] pointed out that the dispersion relation of the propagating modes in this structure is similar to that of the plasmas of electron gas. Moreover, the split ring resonators can have an effectively negative permeability over a microwave frequency band [7–10], and, therefore, the first left-handed metamaterial in microwave frequency was developed. Besides, the extraordinary phenomenon of negative group velocity in a metamaterial was investigated and its correlation to slanted stop-band was verified theoretically [11]. Additionally, some researchers used the effective medium method to consider the metamaterial slab as a uniform medium [12]. The single-mode approximation was employed to extract the effective parameters using the scattering parameters of the metamaterial slab [13]. A metamaterial consisting of six identical metallic grid with a square lattice immersed in foam with relative dielectric constant close to unity was designed to shape the radiation pattern due to a line source embedded in the metamaterial [14]. It is the first time that the antenna design incorporates a wired-based metamaterial for obtaining a directional antenna. Besides, one- and two-dimensional metamaterial structures were designed for directive emission [15]. The experimental and numerical evidence proves that metamaterials can not only modify the emission of an embedded source but also enhance the gain and directivity [16]. A new method to enhance the gain in rectangular and circular waveguide antenna arrays using double negative medium (DNG) structure composed of strip wires and split ing resonators was proposed [17, 18]. Besides, researchers used subwavelength metallic hole arrays to enhance the emission by a focused beam with narrow bandwidth [19]. Researchers [20] used the known grid structure as a highly directive superstrate suspended over a patch antenna and demonstrated its operation with a multi-gigabit per second signal. Moreover, high gain and low-profile electromagnetic band-gap resonator antennas based on frequency-selective-surface (FSS) type metamaterials are studied [21]. Metamaterial superstrate

composed of stacked S-shaped split ring resonators was designed at WiMAX 2.5 GHz band (2.50–2.69 GHz) [22]. A review of the development for high gain antenna design using periodic structures was summarized [23]. Regarding the E-plane horn antenna design, intensive studies in were conducted theoretically and experimentally and reported in the literature. Numerical methods involving geometrical diffraction theory and conventional aperture techniques were employed to analyze the radiation characteristics of E-plane horn antennas [24–26]. The radiation patterns of rectangular electromagnetic horn antennas against the structural parameters such as flare angle and radial length were systematically investigated [27]. Reflection of diffracted fields from the horn interior and double diffraction at the aperture were considered to explain the gain variation observed in a pyramidal horn antenna [28, 29]. A numerical technique solving the hybrid field integral equation (HFIE) by method of moments was developed for electrically large pyramidal horn antennas [30]. Recently, several novel horn antennas of new types were designed and analyzed such as compound box-horn antenna and modified TEM horn antenna [31, 32]. The former one possessed the advantages of both the modified box-horn and pyramidal horn antennas whereas the latter one removed fluctuations introduced by conventional TEM horn antenna by carving an arc shape on the antenna's open end.

In this research, we first synthesize a wire-medium metamaterial invoking the theoretical analysis regarding the phase relation of waves propagating in the metamaterial. Once the frequency range where the effective refractive index is smaller than unity was determined, the antenna structure consisting of the metamaterial and excitation source were put into simulation for obtaining its radiation characteristics. In addition to the numerical simulation, we have fabricated this antenna and measured its radiation pattern using vector network analyzer HP8722D and double-ridged horn antennas. The excellent agreement between the numerical and measured results confirms the design concept of this metamaterial-based E-plane horn antenna.

2. DESCRIPTION OF THIS ANTENNA

As shown in Figure 1, this antenna consists of parallel metallic plates whose four openings are flared in the direction of E-field (along z-axis). Inside the parallel-plate region, there is a metamaterial made up of metallic circular cylinders arranged in a 2D square lattice. The metallic parallel plates are made by aluminum with thickness 1.6 mm. The distance between the parallel plates as well as the height of the

metallic rod are the same and is denoted as $h = 9\,\text{mm}$. Regarding the metamaterial, the number of metallic rods along the x- and y-direction respectively are $N_x = 6$ and $N_y = 6$. Moreover, the periods along the x- and y-direction are $a = 15\,\text{mm}$ and $b = 15\,\text{mm}$, respectively. The metallic circular cylinder has the radius $r = 1.18\,\text{mm}$. The

(a)

(b)

(c)
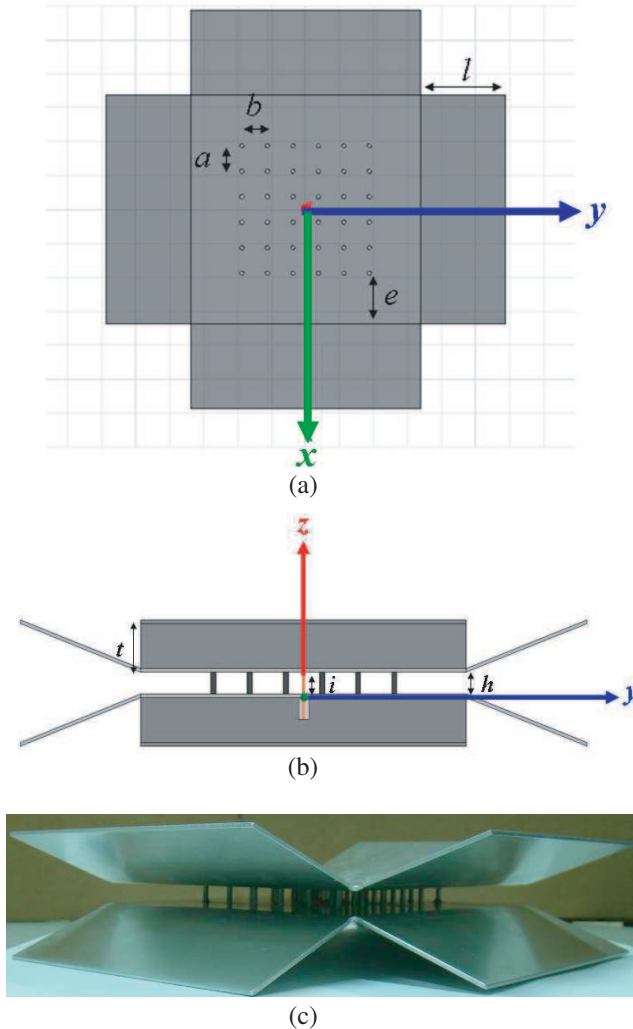
Figure 1. Structure configuration of the metamaterial-based antenna; (a) top view, (b) side view, and (c) photo of this antenna.

distance from the edge of metamaterial to the edge of metal plate is $e = 30\,\text{mm}$. The length and height of the flared opening are $l = 50\,\text{mm}$ and $t = 20\,\text{mm}$, respectively. The structure is fed by a coaxial probe with its center conductor ($i = 8\,\text{mm}$) extending into the parallel-plate region.

3. PHYSICAL BACKGROUND

For a commonly used E-plane horn antenna, the upper and lower walls of the waveguide were tapered to form a large opening. Accordingly, the tapering of the dominant TE_{10} mode from the waveguide to the large aperture results in a high gain radiation pattern. Different from the E-plane horn antenna, in this design we produce almost uniform electric field on each of the flared aperture. Thus, in the azimuth and elevation direction, we could obtain a directional far-field pattern with extremely low side lobes in each sector. Specifically, the uniform electric fields are contributed by the excitation of line-source embedded in the metamaterial sandwiched by the two parallel plates. As will become clear later on, since the phase relation (the relation among k_x, k_y and k_o) of the waves supported in the metamaterial forms a circle with its radius smaller than that of the waves in a uniform medium, the effective refractive index (n_{eff}) is smaller than that in the uniform medium. From Snell's law, we know that the outgoing wave tends to be perpendicular to the interface between metamaterial and uniform regions. Therefore, probe source excites equal power of four ways flowing along the four axes ($+x$, $-x$, $+y$ and $-y$), respectively. After guiding the four waves into each of the flared opening, the directional radiation pattern in respective axis was obtained.

4. NUMERICAL AND EXPERIMENTAL RESULTS

4.1. Dispersion and Phase Relations

As far as a periodic medium is concerned, the dispersion (or phase) relation of the eigen-waves supported in the medium is an important issue to be studied in detail. Since the height between the parallel plates is smaller compared with the size of the metal plate along the x- and y-direction, the electric field is assumed to be uniform along the z-direction. The three-dimensional vector boundary-value problem can be simplified into a two-dimensional scalar one. Therefore, the E_z mode and H_z mode can be handled individually. In this problem, only the E_z mode is excited, so we may assumed that the electric field has no variation along the z-direction. To obtain the phase relation of

wave propagation in the periodic medium, the mode-matching method incorporating the Floquet mode was employed to expand the electric and magnetic fields in each constituent region. By imposing the periodic boundary (or Bloch) condition over the unit cell, the phase relation among k_x, k_y and k_o can be determined.

We have written a computer code for calculating the dispersion relation (the relation among k_x, k_y and k_o) of the metamaterial composed of 2D metallic rods array. Figures 2(a) and 2(b) depict the dispersion- and phase-relation of the waves supported in the metamaterial, respectively. In Figure 2(a), we demonstrate the dispersion relation of the metamaterial medium. Here the k_x is set to zero to calculate the propagation constant along the y-direction (k_y) for a given frequency. Since the structure is assumed to be lossless, the complex number of k_y has complex conjugate roots. We plot their absolute value of the real- and imaginary-part of k_y for easy reference. The lines with blue- and green-color respectively represent the normalized phase ($\beta_y a/2\pi$) and attenuation ($\alpha_y a/2\pi$) constants. It is obvious to see that before 7.2 GHz, the wave is below-cutoff and has considerable attenuation constant. Such a region was usually characterized as a plasma-like region having effective negative permittivity. After the cutoff frequency and below around 10.5 GHz (pass-band region), the wave can propagate. Notice that there is a stop-band with a parabolic shape of attenuation distribution from 10.5 GHz to 14 GHz, which is due to the contra-flow coupling between
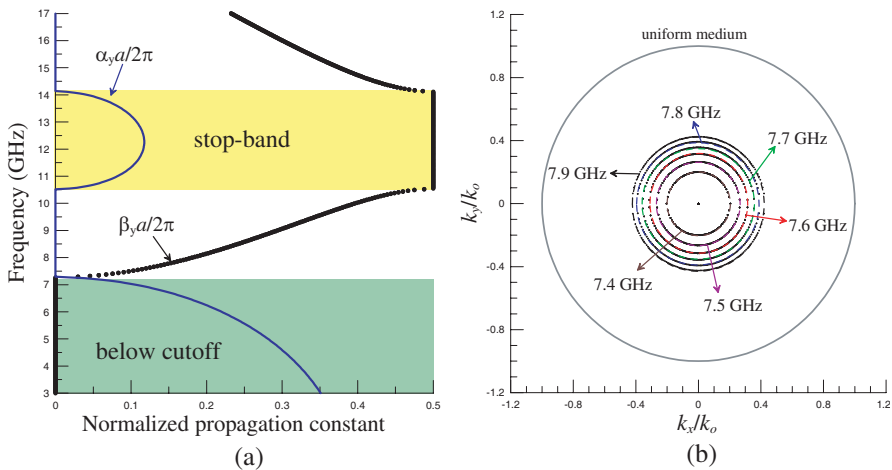

Figure 2. Dispersion relation and phase relation of the metamaterial medium; (a) dispersion relation, and (b) phase relation.

the fundamental and first higher-order space harmonics in the periodic structure.

In Figure 2(b), the horizontal and the vertical axes respectively represent the normalized phase constant (k_x/k_o and k_y/k_o) along the x- and y-axis. The circles in colored lines are those calculated from 7.4 GHz to 7.9 GHz with 0.1 GHz step, while the circle with grey line is the phase relation in uniform parallel-plate region. As is well known, the radius of the circle represents the square root of n_{eff}. Apparently the n_{eff} of the wave in the metamaterial is much smaller than that in the region without metamaterial.

It is noted that the phase relation shown in Figure 2(b) was obtained by giving a real number of k_x to calculate the eigen-value k_y. Actually, k_y may be real number or complex number. The k_y outside the circle is a complex number with pure imaginary. Namely, if the k_x is outside the circle, the wave experiences a strong reflection due to the large attenuation constant. Moreover, since the structure of the metal-material is symmetric, for a given k_y, we may obtain the same distribution of phase relation as shown in Figure 2(a).

After understanding the characteristics of eigen-waves propagating in the metamaterial, we are now in a good position to explore the extraordinary refraction in the structure consisting of the metamaterial. By properly tuning the length of the monopole (line source) in the metamaterial, we can excite the wave having effective refractive index smaller than unity. Therefore, the refractive waves shall be normal to
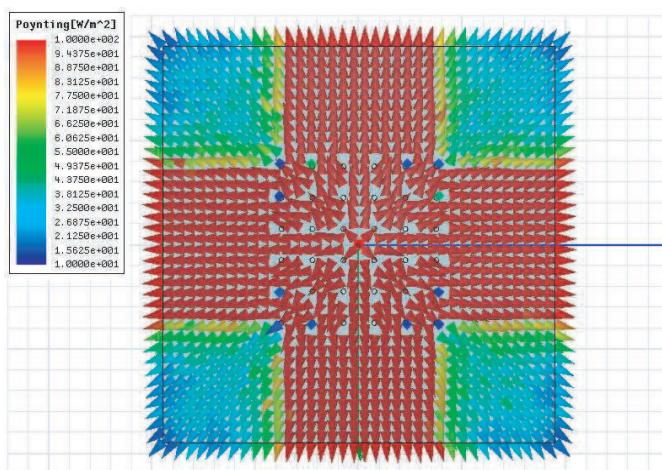

Figure 3. Poynting power distribution within the parallel-plate region (7.5 GHz) with metamaterial.

the metamaterial surface. To confirm the truth of the conjecture, we calculated the vector Poynting power distribution for demonstrating the power flow. As shown in Figure 3, the refracted wave leaving the metamaterial boundary tends to be perpendicular to the interface, in particular for those around the central part of each boundary, while the others propagates at a small angle deviated from the direction perpendicular to the boundary.

Figure 4 depicts the reflection coefficient (S_{11}) of this antenna. The line with symbols is the simulation result using a finite-integration-based code (CST Microwave Studio), while the line without symbols represents the measured result. Since this structure does not contain any dielectric medium and the metallic loss is not significant in the frequency band of operation, the low return loss from around 7.35 GHz to 7.58 GHz represents that most of the input power is radiated by this antenna. Moreover, this antenna is intended for designing in this band because the metamaterial is operated in the condition that n_{eff} is smaller than unity. Besides, we have changed the length of the monopole to see the effect on the return loss of this antenna. As shown in Figure 5, the length of the monopole can alter the center frequency of the return response. Since the frequency range where the effective refractive index is smaller than unity is dependent on the unit cell parameters, we can properly change the length of the monopole to excite the wave with $n_{eff} \ll 1$.
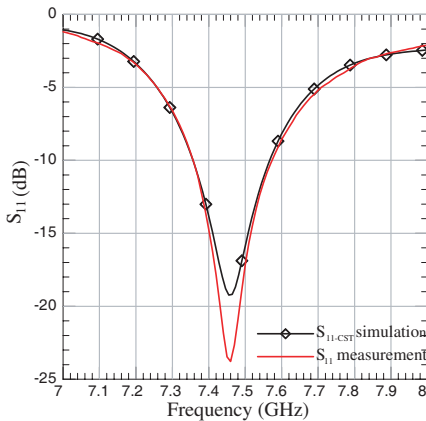
Figure 4. Reflection coefficient (in dB) versus frequency of this antenna.
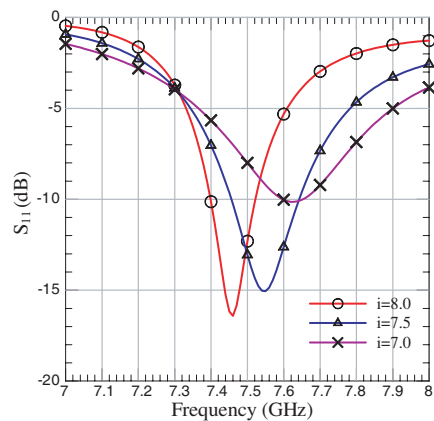
Figure 5. Simulated S_{11} versus frequency for various i, the length of center conductor extending into the parallel-plate region.
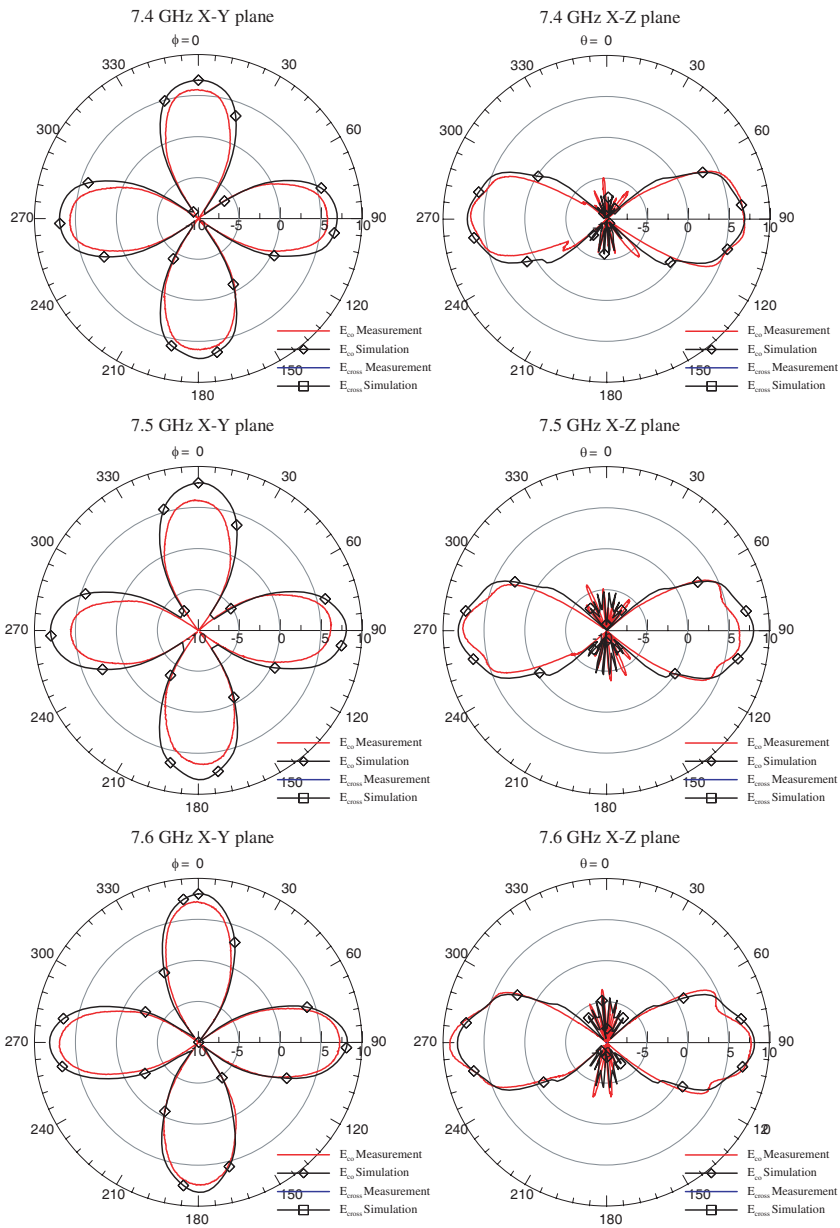
Figure 6. Radiation patterns in the elevation plane and azimuth plane.

4.2. Radiation Characteristics

Figure 6 shows the radiation pattern along the azimuth (X-Y) plane and elevation (X-Z) plane, respectively, for the operation frequencies from 7.4 GHz to 7.6 GHz with 0.1 GHz step. For each frequency, the radiation pattern was obtained with an angle resolution of $2\pi/1400$ radian. From these figures shown in Figure 6, it is apparent to observe that there are four directional beam patterns in the four sectors. It is noted that the measured antenna gain has been calibrated by that of the standard horn antenna.

To facilitate the understanding for the performance of this antenna, the measured results of antenna gain, side-lobe level (SLL) and half-power beam width (HPBW) were listed in Tab. 1. Comparing the patterns between the azimuth and elevation planes, we found that the pattern in X-Z plane has the wider 3-dB beam-width than that of the X-Y plane because of the smaller dimension of the flared opening along the z-direction than that in the x- (or y-) direction. Additionally, the cross-polarization component in X-Y and X-Z plane is much smaller than that of the co-polarization. Therefore, in Figure 6, the cross-polarization can not be seen. Figure 7 depicts measured- and simulated-gain form 7.4 GHz to 7.9 GHz with 0.1 GHz step. Notably, this antenna has at least 6 dB gain in the frequency range of operation.

To demonstrate the function of the metamaterial, the antenna without the metamaterial was considered to carry out the calculation for its radiation pattern. The radiation patterns for the frequency
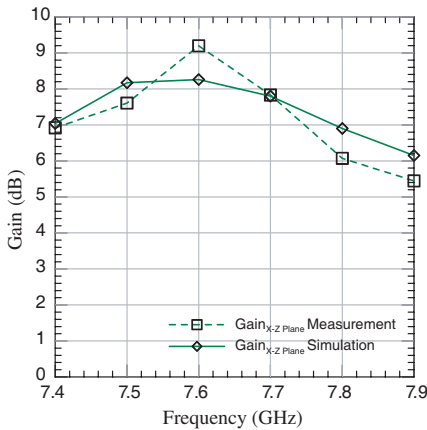
Figure 7. Maximum gain of measured and simulated results versus frequency.
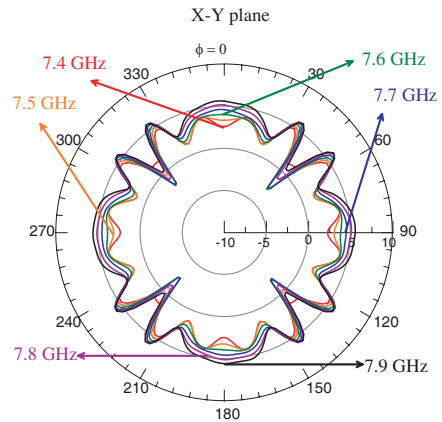
Figure 8. Radiation patterns of this horn antenna without metamaterial.

ranging from 7.4 GHz to 7.9 GHz were plotted in Figure 8. Besides, we can also see the great enhancement in side-lobe level from Tab. 2. As was conjectured from the physical intuition, the line source excites outgoing cylindrical waves in the air region. Since the wave front on each of the flared aperture is not uniform, the radiation pattern is not a directional one. Consequently, the radiation from the regions without flared opening is significant because that the cylindrical wave can propagate in all direction.

Table 1. Measured antenna performance in X-Y plane and X-Z plane.

X-Y plane (co-polarization)						
Frequency (GHz)	7.4	7.5	7.6	7.7	7.8	7.8
Max. gain (dB)	6.92	7.61	9.20	7.83	6.07	5.44
SLL (dB)	−15.14	−17.39	−21.60	−21.12	−16.11	−12.23
HPBW (degree)	37.36°	33.76°	30.02°	26.91°	25.60°	25.31°
X-Z plane (co-polarization)						
Frequency (GHz)	7.4	7.5	7.6	7.7	7.8	7.8
Max. gain (dB)	6.92	7.61	9.20	7.83	6.07	5.44
SLL (dB)	−11.86	−11.48	−12.37	−11.55	−9.16	−8.82
HPBW (degree)	45.11°	42.28°	35.61°	31.24°	29.68°	29.74°

Table 2. Comparison between E-plane horn antennas with and without metallic wires.

X-Y plane (co-polarization)						
Frequency (GHz)	7.4	7.5	7.6	7.7	7.8	7.9
Main beam (dB) $\phi = 34°$	4.84	5.22	5.55	5.78	5.84	5.69
Sidelobe (dB) $\phi = 0°$	2.58	3.33	4.00	4.60	5.15	5.60
SLL w/o MTM (dB)	−2.26	−1.89	−1.55	−1.18	−0.69	−0.09
SLL with MTM (dB)	−15.14	−17.39	−21.60	−21.12	−16.11	−12.23
Enhanced SLL (dB)	12.88	15.50	20.05	19.94	15.42	12.14

5. CONCLUSION

In this research, we employed a metamaterial in an E-plane horn antenna design. Through the rigorous calculation for the phase relation of the wave in such a metamaterial, we can synthesize a medium having an effective refractive index smaller than unity. Thus, the power flow leaving the metamaterial tends to be perpendicular to the interface between uniform medium and metamaterial. In fact, such a metamaterial can have the function of a 4-way power divider which equally distributes the input signal into 4 ways along the 4 different directions. Accordingly, we respectively guide those refractive beams into flared openings to radiate directional beam in each sector. We obtained an excellent agreement between the measured and simulated results. This antenna is applicable to point-to-multiple-point downlink systems due to its robust, low-loss and low-cost properties. This antenna is designed for the downlink applications related to an experimental network in our campus. We implemented this antenna at the center position of each floor in a large building. Through the beam-splitting property of this antenna, the access point in each wing of a large building received respectively the transmitting data. Furthermore, access points relay the signal to the users via the wired or wireless local network. Although we demonstrated the performance of this antenna around 7.4 GHz, it is easy for scaling the structure to any desired frequency of applications.

ACKNOWLEDGMENT

REFERENCES

1. Engheta, N. and R. W. Ziolkowski, "Introduction, history and fundamental theories of double-negative (DNG) metamaterials," *Metamaterials: Physics and Engineering Explorations*, Chap. 1, 5–41, IEEE Press, John Wiley & Sons, Inc., June 2006.
2. Engheta, N., A. Alu, R. W. Ziolkowski, and A. Erontok, "Fundamentals of waveguides and antenna applications involving double-negative (DNG) and single-negative (SNG) metamaterials," *Metamaterials: Physics and Engineering Explorations*, Chap. 2, 43–85, IEEE Press, John Wiley & Sons, Inc., June 2006.

3. Ding, W., L. Chen, and C. H. Liang, "Characteristics of electromagnetic wave propagation in biaxial anisotropic left-handed materials," *Progress In Electromagnetics Research*, PIER 70, 37–52, 2007.

4. Grzegorczyk, T. M., X. Chen, J. Pacheco, J. Chen, B. I. Wu, and J. A. Kong, "Reflection coefficients and Goos-Hanchen shifts in anisotropic and bianisotropic left-handed metamaterials," *Progress In Electromagnetics Research*, PIER 51, 83–113, 2005.

5. Pendry, J. B., A. J. Holden, D. J. Robbins, and W. J. Stewart, "Low frequency plasmons in thin-wire structures," *J. Phys. Condens. Matter*, Vol. 10, No. 22, 4785–4809, 1998.

6. Hudlicka, M., J. Machac, and I. S. Nefedov, "A triple wire medium as an isotropic negative permittivity metamaterial," *Progress In Electromagnetics Research*, PIER 65, 233–246, 2006.

7. Pendry, J. B., A. J. Holden, D. J. Robbins, and W. J. Stewart, "Magnetism from conductors and enhanced nonlinear phenomena," *IEEE Trans. Microwave Theory Tech.*, Vol. 47, No. 11, 2075–2084, Nov. 1999.

8. Xi, S., H. Chen, B.-I. Wu, and J. A. Kong, "Experimental confirmation of guidance properties using planar anisotropic left-handed metamaterial slabs based on S-Ring Resonators," *Progress In Electromagnetics Research*, PIER 84, 279–287, 2008.

9. Wongkasem, N., A. Akyurtlu, J. Li, A. Tibolt, Z. Kang, and W. D. Goodhue, "Novel broadband terahertz negative refractive index metamaterials: Analysis and experiment," *Progress In Electromagnetics Research*, PIER 64, 205–218, 2006.

10. Shelby, R. A., D. R. Smith, and S. Schultz, "Experimental verification of a negative index of refraction," *Science*, Vol. 292, 77–79, Apr. 2001.

11. Hwang, R. B., "Relations between the reflectance and band structure of 2D metallo-dielectric electromagnetic crystals," *IEEE Transactions on Antennas and Propagation*, Vol. 52, No. 6, 1454–1464, June 2004.

12. Li, C., Q. Sui, and F. Li, "Complex guided wave solution of grounded dielectric slab made of metamaterials," *Progress In Electromagnetics Research*, PIER 51, 187–195, 2005.

13. Chen, X., T. M. Grzegorczyk, B.-I. Wu, J. Pacheco, and J. A. Kong, "Robust method to retrieve the constitutive effective parameters of metamaterials," *Phys. Rev. E*, Vol. 70, No. 1, 016608, 2004.

14. Enoch, S., G. Tayeb, P. Sabouroux, N. Guerin, and P. Vincent,

"A metamaterial for directive emission," *Phys. Rev. Lett.*, Vol. 89, No. 21, 213902, Nov. 2002.

15. Weng, Z.-B., Y.-C. Jiao, G. Zhao, and F.-S. Zhang, "Design and experiment of one dimension and two dimension metamaterial structures for directive emission," *Progress In Electromagnetics Research*, PIER 70, 199–209, 2007.

16. Wu, B.-I., W. Wang, J. Pacheco, X. Chen, T. M. Grzegorczyk, and J. A. Kong, "A study of using metamaterials as antenna substrate to enhance gain," *Progress In Electromagnetics Research*, PIER 51, 295–328, 2005.

17. Liang, L., B. Li, S. H. Liu, and C. H. Liang, "A study of using the double negative structure to enhance the gain of rectangular waveguide antenna arrays," *Progress In Electromagnetics Research*, PIER 65, 275–286, 2006.

18. Li, B., B. Wu, and C.-H. Liang, "Study on high gain circular waveguide array antenna with metamaterial structure," *Progress In Electromagnetics Research*, PIER 60, 207–219, 2006.

19. Beruete, M., I. Campillo, J. E. Rodríguez-Seco, E. Perea, M. Navarro-Cía, I. J. Núñez-Manrique, and M. Sorolla, "Enhanced gain by double-periodic stacked subwavelength hole array," *IEEE Microwave and Wireless Components Letters*, Vol. 17, No. 12, 831–833, Dec. 2007.

20. Franson, S. J. and R. W. Ziolkowski, "Gigabit per second data transfer at 60 GHz in high gain grid antennas," *IEEE AP-S*, Jul. 2008.

21. Yuehe, G. and K. P. Esselle, "High-gain, low-profile EBG resonator antennas with very thin metamaterial superstrates," *IEEE AP-S*, Jul. 2008.

22. Lin, H.-H., C.-Y. Wu, and S.-H. Yeh, "Metamaterial enhanced high gain antenna for WiMAX application," *IEEE AP-S*, Oct. 2007.

23. Vardaxoglou, Y. and F. Capolino, "Review of highly-directive flat-plate antenna technology with metasurfaces and metamaterials," *IEEE Proceedings of the 36th European Microwave Conference*, 963–966, Sept. 2006.

24. Russo, P., R. Rudduck, and L. Peters, Jr., "A method for computing E-plane patterns of horn antennas," *IEEE Trans. Antennas and Propagation*, Vol. 13, No. 2, 219–224, Mar. 1965.

25. Safaai-Jazi, A. and E. Jull, "A short horn with high E-plane directivity," *IEEE Trans. Antennas and Propagation*, Vol. 25, No. 6, 854–859, Nov. 1977.

26. Yu, J., R. Rudduck, and L. Peters, Jr., "Comprehensive analysis for E-plane of horn antennas by edge diffraction theory," *IEEE Trans. Antennas and Propagation*, Vol. 14, No. 2, 138–149, Mar. 1966.

27. Rhodes, D. R., "An experimental investigation of the radiation patterns of electromagnetic horn antennas," *Proceedings of the IRE*, Vol. 36, No. 9, 1101–1105, Sept. 1948.

28. Jull, E., "Errors in the predicted gain of pyramidal horns," *IEEE Trans. Antennas and Propagation*, Vol. 21, No. 1, 25–31, Jan. 1973.

29. Jull, E., "Reflection from the aperture of a long E-plane sectoral horn," *IEEE Trans. Antennas and Propagation*, Vol. 20, No. 1, 62–68, Jan. 1972.

30. Liu, K., C. A. Balanis, C. R. Birtcher, and G. C. Barber, "Analysis of pyramidal horn antennas using moment methods," *IEEE Trans. Antennas and Propagation*, Vol. 41, No. 10, 1379–1389, Oct. 1993.

31. Gupta, R. C., "Analysis of radiation patterns of compound boxhorn antenna," *Progress In Electromagnetics Research*, PIER 76, 31–34, 2007.

32. Mallahzadeh, A. R. and F. Karshenas, "Modified TEM horn antenna for broadband applications," *Progress In Electromagnetics Research*, PIER 90, 105–119, 2009.